AIAA 81-0632R

Large-Amplitude Random Response of Angle-Ply Laminated Composite Plates

Chuh Mei*
Old Dominion University, Norfolk, Virginia
and
Kenneth R. Wentz†
Air Force Wright Aeronautical Laboratories, Wright-Patterson Air Force Base, Ohio

Large-amplitude response of antisymmetric angle-ply laminated rectangular panels subjected to broadband random acoustic excitation is studied analytically. The boundary conditions considered are all the edges simply supported and all the edges clamped. Inplane edges considered are immovable and movable for each of the cases. Mean-square deflections, mean-square strains/stresses, and equivalent linear frequencies at various acoustic loadings are obtained for laminates of different length-to-width ratios, lamination angles, number of layers, and panel damping ratios. Results obtained can be used as a guide for sonic fatigue design of angle-ply laminates under high noise environment.

Nomenclature

a,b = plate length and width
A,B,D = laminate stiffnesses, Eq. (8)
err = error of linearization, Eq. (42)
$E[q^2]$ = mean-square of q, Eq. (47)
E_1,E_2 = Young's moduli in major (longitudinal) and minor (transverse) principal material directions
f = equivalent linear frequency, Hz
F = stress function, Eq. (11)
G_{12} = shear modulus
h = plate thickness
$H(\omega)$ = frequency response function, Eq. (48)
m = mass coefficient, Eqs. (26a) and (37a)
M = resultant bending moment per unit width
n = number of layers
N = resultant normal force per unit width
$\bar{N}_x,\bar{N}_y$ = constants, Eqs. (29) and (38)
p = pressure
q = modal amplitude or displacement
r = length-to-width ratio, a/b
S = nondimensional excitation spectral density parameter, Eq. (51)
$S_p(\omega)$ = spectral density function of excitation pressure $p(t)$
t = time
u,v,w = displacements
x,y,z = coordinates
β = nonlinearity coefficient
β^* = nondimensional nonlinearity coefficient
ϵ,γ = strains
ζ = damping ratio, c/c_c
θ = lamination angle
κ = middle surface curvature
λ = nondimensional frequency parameter
$\phi(F,w)$ = function, Eq. (13c)
ω = frequency, rad/s
Ω = equivalent linear or nonlinear frequency, rad/s

Subscripts

c = complementary solution
p = particular solution
x,y,z = coordinate directions
0 = linear

Superscript

k = kth layer

I. Introduction

THE need to improve sonic fatigue resistance of aircraft structures has become increasingly important as a result of military and commercial demands on current and future airplane designs. Numerous theoretical studies[1-6] and experimental investigations[7-12] on sonic fatigue design of aircraft structures have been undertaken during the past several years to help provide the needed reliability.

The majority of analytical investigations to date have been formulated within the framework of linear or small-deflection structural theory. Test results on various aircraft panels in Refs. 5, 7, and 9-12, however, have shown that high noise levels in excess of 120 dB produce nonlinear behavior with large deflections in such panels. The linear analyses often predict the root-mean-square (rms) deflection and rms strains/stresses well above those of the experiment, and the frequencies of vibration well below those of the experiment.[7,11,12] It is known that the prediction of service/fatigue life is based on rms stress/strain and predominant response frequency in conjunction with the stress vs cycles to failure (S-N) data. Current analytical design methods[2,4,5,7] for sonic fatigue prevention are based essentially on linear theory. The use of linear analyses, therefore, would lead to poor estimation of panel fatigue life.

High modulus-type fiber-reinforced composite materials are under development for use on aircraft components such as skin panels, substructural parts, etc. Many of these structural components are exposed to high-intensity noise fields generated by the aircraft propulsion system and are subjected to acoustic fatigue. However, few investigations on large-amplitude random response of composite plates are reported in the literature. In the present paper, the large deflection response of regular antisymmetric angle-ply laminated rectangular plates subjected to broadband random acoustic excitation is studied analytically. The boundary conditions considered are all the edges simply supported and all the edges clamped. Inplane edges considered are immovable and movable for each of the preceding cases. The classical Kir-

Presented as Paper 81-0632 at the AIAA/ASME/ASCE/AHS 22nd Structures, Structural Dynamics and Materials Conference, Atlanta, Ga., April 6-8, 1981; submitted April 24, 1981; revision received Feb. 22, 1982.

*Associate Professor, Department of Mechanical Engineering and Mechanics. Member AIAA.
†Aerospace Engineer, Acoustics and Sonic Fatigue Group.

chhoff hypothesis and the Karman-type geometric nonlinearity are used in the formulation. Thin-plate equations for angle-ply laminates in terms of a stress function and the deflection function are derived. A deflection function satisfying the out-of-plane boundary condition is assumed. Corresponding to the assumed mode, a stress function satisfying the different inplane edge conditions is obtained. Galerkin's method is then applied to the governing equation in deflection to yield a nonlinear differential equation with time as the independent variable. The acoustic excitation is assumed to be Gaussian. The equivalent linearization method[13-15] is employed so that this nonlinear equation is linearized to an equivalent linear differential equation. An iterative procedure is introduced to obtain rms amplitude and equivalent linear (or nonlinear) frequencies for rectangular laminates of different length-to-width ratios, lamination angles, number of layers, panel damping ratios, and excitation pressure spectral density (PSD). rms strains/stresses are also obtained as a function of rms amplitude.

II. Equations of Motion

The Kirchhoff hypothesis of classical thin-plate theory and the Karman-type geometric nonlinearity lead to the total strains

$$\epsilon_x = \epsilon_x^0 + z\kappa_x \tag{1a}$$

$$\epsilon_y = \epsilon_y^0 + z\kappa_y \tag{1b}$$

$$\gamma_{xy} = \gamma_{xy}^0 + z\kappa_{xy} \tag{1c}$$

where

$$\epsilon_x^0 = u_{,x} + w_{,x}^2/2 \tag{2a}$$

$$\epsilon_y^0 = v_{,y} + w_{,y}^2/2 \tag{2b}$$

$$\gamma_{xy}^0 = u_{,y} + v_{,x} + w_{,x}w_{,y} \tag{2c}$$

With the assumption of small slopes ($w_{,x}^2 \ll 1$ etc.), the middle surface curvatures can be written as

$$\kappa_x = -w_{,xx} \qquad \kappa_y = -w_{,yy} \qquad \kappa_{xy} = -2w_{,xy} \tag{3}$$

The plate equations are obtained by applying d'Alembert's principle to an element of the kth layer of the laminate. Integrating these equations over the plate thickness h, neglecting inplane inertia and rotary inertia terms, and retaining those nonlinear terms in accordance with the von Kármán assumptions, lead to the following equations of motion:

$$N_{x,x} + N_{xy,y} = 0 \qquad N_{xy,x} + N_{y,y} = 0 \tag{4}$$

$$M_{x,xx} + 2M_{xy,xy} + M_{y,yy} + N_x w_{,xx} + 2N_{xy} w_{,xy} + N_y w_{,yy} + p = \rho h \ddot{w} \tag{5}$$

where the average mass density of the laminate is defined by

$$\rho = \int_{-h/2}^{h/2} \rho_0^{(k)}\, dz \tag{6}$$

The constitutive relation for a laminated composite plate is[16,17]

$$\begin{Bmatrix} N \\ M \end{Bmatrix} = \begin{bmatrix} A & B \\ B & D \end{bmatrix} \begin{Bmatrix} \epsilon^0 \\ \kappa \end{Bmatrix} \tag{7}$$

The laminate stiffnesses A, B, and D are symmetric matrices defined by the relations

$$(A_{ij}, B_{ij}, D_{ij}) = \int_{-h/2}^{h/2} (1, z, z^2)\, \bar{Q}_{ij}\, dz \tag{8}$$

The $\bar{Q}_{ij}$ are the transformed reduced stiffness components and can be related to the more familiar engineering elastic moduli. For a regular antisymmetric angle-ply laminated plate, $A_{16} = A_{26} = B_{11} = B_{12} = B_{22} = B_{66} = D_{16} = D_{26} = 0$. Nonvanishing elements of A, B, and D and $\bar{Q}_{ij}$ are given in Refs. 16 and 17. Equation (7) can be rewritten as

$$\begin{Bmatrix} \epsilon^0 \\ M \end{Bmatrix} = \begin{bmatrix} A^* & B^* \\ -(B^*)^T & D^* \end{bmatrix} \begin{Bmatrix} N \\ \kappa \end{Bmatrix} \tag{9}$$

where

$$A^* = A^{-1} \qquad B^* = -A^*B \qquad D^* = D + BB^* \tag{10}$$

Nonvanishing components of the inverted laminate stiffnesses A^*, B^*, and D^* are also given in Ref. 16.

The Airy stress function F is defined such that

$$N^T = \{F_{,yy} \quad F_{,xx} \quad -F_{,xy}\} \tag{11}$$

Using Eqs. (3), (7), (9), and (11) in Eq. (5) leads to the equation of motion in the transverse direction as

$$\rho h \ddot{w} + L_1 w - L_3 F - \phi(F, w) - p = 0 \tag{12}$$

where

$$L_1 = D_{11}^* \frac{\partial^4}{\partial x^4} + 2(D_{12}^* + 2D_{66}^*) \frac{\partial^4}{\partial x^2 \partial y^2} + D_{22}^* \frac{\partial^4}{\partial y^4} \tag{13a}$$

$$-L_3 = (2B_{26}^* - B_{61}^*) \frac{\partial^4}{\partial x^3 \partial y} + (2B_{16}^* - B_{62}^*) \frac{\partial^4}{\partial x \partial y^3} \tag{13b}$$

$$\phi(F, w) = F_{,yy} w_{,xx} + F_{,xx} w_{,yy} - 2F_{,xy} w_{,xy} \tag{13c}$$

The compatibility equation is derived from Eq. (2) and is

$$\epsilon_{x,yy}^0 + \epsilon_{y,xx}^0 - \gamma_{xy,xy}^0 + \tfrac{1}{2}\phi(w, w) = 0 \tag{14}$$

By use of Eqs. (9), (11) and (14), the compatibility equation can now be written

$$L_2 F + L_3 w + \tfrac{1}{2}\phi(w, w) = 0 \tag{15}$$

where

$$L_2 = A_{22}^* \frac{\partial^4}{\partial x^4} + (2A_{12}^* + A_{66}^*) \frac{\partial^4}{\partial x^2 \partial y^2} + A_{11}^* \frac{\partial^4}{\partial y^4} \tag{16}$$

Equations (12) and (15) are the governing equations which will be solved by employing Galerkin's approach and the equivalent linearization method.

III. Method of Analysis

A. Simply Supported Angle-Ply Laminates with Movable Edges

Consider a rectangular angle-ply composite plate of dimensions a, b shown in Fig. 1. The simply supported boundary conditions are

$$x = \pm a/2: \quad w = 0 \quad D_{11}^* w_{,xx} + D_{12}^* w_{,yy} + B_{16}^* N_{xy} = 0 \tag{17a}$$

$$y = \pm b/2: \quad w = 0 \quad D_{12}^* w_{,xx} + D_{22}^* w_{,yy} + B_{62}^* N_{xy} = 0 \tag{17b}$$

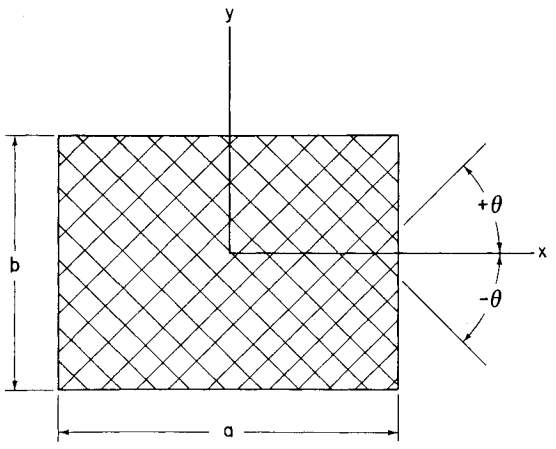

Fig. 1 Angle-ply laminated plate.

For the inplane condition of zero shear stress at the edges, the deflection function satisfying the preceding conditions is assumed as

$$w = q(t)h\cos(\pi x/a)\cos(\pi y/b) \tag{18}$$

Substitution of Eq. (18) into Eq. (15) and solution of the resulting equation leads to the stress function

$$F = F_c + F_p \tag{19}$$

$$F_p = -qhF_{00}\sin\frac{\pi x}{a}\sin\frac{\pi y}{b} - \frac{q^2h^2r^2}{32}\left(F_{10}\cos\frac{2\pi x}{a} + F_{01}\cos\frac{2\pi y}{b}\right) \tag{20}$$

where the constants F_{ij} are

$$F_{00} = \frac{(2B^*_{26} - B^*_{61})r + (2B^*_{16} - B^*_{62})r^3}{A^*_{22} + (2A^*_{12} + A^*_{66})r^2 + A^*_{11}r^4} \tag{21a}$$

$$F_{10} = 1/A^*_{22} \qquad F_{01} = 1/A^*_{11}r^4 \tag{21b}$$

The complementary solution F_c will now be obtained such that it satisfies inplane boundary conditions. For movable edges corresponding to case S4 in Ref. 18, the inplane boundary conditions are

$$x = \pm a/2: \quad F_{,xy} = 0 \qquad \int_{-b/2}^{b/2} F_{,yy}\,dy = 0 \tag{22a}$$

$$y = \pm b/2: \quad F_{,xy} = 0 \qquad \int_{-a/2}^{a/2} F_{,xx}\,dx = 0 \tag{22b}$$

Because of these conditions, F_c can be shown to be zero; hence, $F = F_p$.

With the assumed deflection w given by Eq. (18) and stress function F given by Eq. (20), Eq. (12) is then satisfied by applying Galerkin's method:

$$\iint[\rho h\ddot{w} + L_1 w - L_3 F - \phi(F,w) - p]\,w\,dx\,dy = 0 \tag{23}$$

which yields a modal equation of the form

$$\ddot{q} + \omega_0^2 q + \beta_p q^3 = p(t)/m \tag{24}$$

and

$$\omega_0^2 = \lambda_0^2(E_2h^2/\rho b^4) \qquad \beta_p = \beta_p^*(E_2h^2/\rho b^4) \tag{25}$$

$$m = \pi^2\rho h^2/16 \tag{26a}$$

$$\lambda_0^2 = \frac{\pi^4}{E_2h^3r^4}\{D^*_{11} + 2(D^*_{12} + 2D^*_{66})r^2 + D^*_{22}r^4 + F_{00}[(2B^*_{26} - B^*_{61})r + (2B^*_{16} - B^*_{62})r^3]\} \tag{26b}$$

$$\beta_p^* = \frac{\pi^4}{16E_2h}(F_{10} + F_{01}) \tag{26c}$$

B. Simply Supported Angle-Ply Laminates with Immovable Edges

The inplane boundary conditions corresponding to case S3 in Ref. 18 are

$$x = \pm a/2: \quad F_{,xy} = 0 \quad \iint(\epsilon_x^0 - \tfrac{1}{2}w_{,x}^2)\,dx\,dy = 0 \tag{27a}$$

$$y = \pm b/2: \quad F_{,xy} = 0 \quad \iint(\epsilon_y^0 - \tfrac{1}{2}w_{,y}^2)\,dx\,dy = 0 \tag{27b}$$

The complementary solution is assumed as

$$F_c = \bar{N}_y(x^2/2) + \bar{N}_x(y^2/2) \tag{28}$$

It follows from Eqs. (9), (18), (27), and (28) that

$$\bar{N}_x = \frac{q^2h^2\pi^2}{8(A^*_{11}A^*_{22} - A^{*2}_{12})}\left(\frac{A^*_{22}}{a^2} - \frac{A^*_{12}}{b^2}\right) \tag{29a}$$

$$\bar{N}_y = \frac{q^2h^2\pi^2}{8(A^*_{11}A^*_{22} - A^{*2}_{12})}\left(\frac{A^*_{11}}{b^2} - \frac{A^*_{12}}{a^2}\right) \tag{29b}$$

The particular solution F_p has been obtained and given in Eq. (20). The total stress function, therefore, is $F = F_c + F_p$. Substitution of the stress function F and the deflection w in Eq. (23) yields

$$\ddot{q} + \omega_0^2 q + (\beta_p + \beta_c)q^3 = p(t)/m \tag{30}$$

where

$$\beta_c = \beta_c^*(E_2h^2/\rho b^4) \tag{31a}$$

$$\beta_c^* = \frac{\pi^4}{8E_2hr^4}\left(\frac{A^*_{22} - 2A^*_{12}r^2 + A^*_{11}r^4}{A^*_{11}A^*_{22} - A^{*2}_{12}}\right) \tag{31b}$$

The term β_c is an addition to the nonlinearity coefficient due to immovable inplane edges.

C. Clamped Angle-Ply Laminates with Movable Edges

The deflection function which satisfies the clamped condition on all four edges of the plate is assumed as

$$w = \frac{qh}{4}\left(1 + \cos\frac{2\pi x}{a}\right)\left(1 + \cos\frac{2\pi y}{b}\right) \tag{32}$$

Introducing Eq. (32) in Eq. (15) and solving for F yields

$$F = F_c + F_p \tag{33}$$

$$F_p = -\frac{qh}{4}F_{00}\sin\frac{2\pi x}{a}\sin\frac{2\pi y}{b} - \frac{q^2h^2r^2}{32}\left(F_{10}\cos\frac{2\pi x}{a} + F_{01}\cos\frac{2\pi y}{b} + F_{11}\cos\frac{2\pi x}{a}\cos\frac{2\pi y}{b} + F_{20}\cos\frac{4\pi x}{a} + F_{02}\cos\frac{4\pi y}{b} + F_{21}\cos\frac{4\pi x}{a}\cos\frac{2\pi y}{b} + F_{12}\cos\frac{2\pi x}{a}\cos\frac{4\pi y}{b}\right) \tag{34}$$

where the constants F_{ij} are

$$F_{00} = \frac{(2B^*_{26} - B^*_{61})r + (2B^*_{16} - B^*_{62})r^3}{A^*_{22} + (2A^*_{12} + A^*_{66})r^2 + A^*_{11}r^4} \tag{35a}$$

$$F_{10}=1/A_{22}^* \qquad F_{01}=1/A_{11}^* r^4 \tag{35b}$$

$$F_{11}=\frac{2}{A_{22}^*+(2A_{12}^*+A_{66}^*)r^2+A_{11}^* r^4} \tag{35c}$$

$$F_{20}=1/16A_{22}^* \qquad F_{02}=1/16A_{11}^* r^4 \tag{35d}$$

$$F_{21}=\frac{1}{16A_{22}^*+4(2A_{12}^*+A_{66}^*)r^2+A_{11}^* r^4} \tag{35e}$$

$$F_{12}=\frac{1}{A_{22}^*+4(2A_{12}^*+A_{66}^*)r^2+16A_{11}^* r^4} \tag{35f}$$

Because of the movable inplane edge conditions Eq. (22) (case C4 in Ref. 18), F_c can be shown to be zero; hence, $F=F_p$. Introducing the expressions for w and F in Eq. (23) yields

$$\ddot{q}+\omega_0^2 q+\beta_p q^3=p(t)/m \tag{36}$$

where ω_0 and β_p have been defined in Eq. (25), and

$$m=9\rho h^2/16 \tag{37a}$$

$$\lambda_0^2=\frac{16\pi^4}{9E_2h^3r^4}\{3D_{11}^*+2(D_{12}^*+2D_{66}^*)r^2+3D_{22}^* r^4 + F_{00}[(2B_{26}^*-B_{61}^*)r+(2B_{16}^*-B_{62}^*)r^3]\} \tag{37b}$$

$$\beta_p^*=\frac{\pi^4}{9E_2h}[F_{10}+F_{01}+F_{11}+F_{20}+F_{02}+\tfrac{1}{2}(F_{21}+F_{12})] \tag{37c}$$

D. Clamped Angle-Ply Laminates with Immovable Edges

The complementary stress function is assumed as the form appearing in Eq. (28). Upon enforcing the inplane edge conditions Eq. (27) (case C3 in Ref. 18) yields

$$\bar{N}_x=\frac{3q^2h^2\pi^2}{32(A_{11}^*A_{22}^*-A_{12}^{*2})}\left(\frac{A_{22}^*}{a^2}-\frac{A_{12}^*}{b^2}\right) \tag{38a}$$

$$\bar{N}_y=\frac{3q^2h^2\pi^2}{32(A_{11}^*A_{22}^*-A_{12}^{*2})}\left(\frac{A_{11}^*}{b^2}-\frac{A_{12}^*}{a^2}\right) \tag{38b}$$

Using Eqs. (28), (32), and (38), and applying Galerkin's method yields the modal equation

$$\ddot{q}+\omega_0^2 q+(\beta_p+\beta_c)q^3=p(t)/m \tag{39}$$

The additional nonlinearity coefficient given in Eq. (31) holds also for the clamped case.

E. Damping Factor

Two methods commonly used for determining the damping characteristics of structures are the bandwidth method and the decay rate method. In the bandwidth method, the half-power bandwidth ($=2\zeta$) is measured at modal resonance. In the decay rate method, the logarithmic decrement ($=2\pi\zeta$) of decaying modal response traces is measured. The values of damping ratio ζ ($=c/c_c$) generally range from 0.005 to 0.05 for the common type of composite panel construction used in aircraft structures.[4,12,19] Once the damping ratio is determined from experiments or from existing data of similar construction, the modal equations [Eqs. (24), (30), (36), and (39)] for various boundary conditions can be expressed in a general form as

$$\ddot{q}+2\zeta\omega_0\dot{q}+\omega_0^2 q+\beta q^3=p(t)/m \tag{40}$$

The method of equivalent linearization will be used to obtain an approximate rms amplitude from Eq. (40).

F. Method of Equivalent Linearization

The basic idea of the equivalent linearization method is to assume that an approximate solution to Eq. (40) can be obtained from the linearized equation

$$\ddot{q}+2\zeta\omega_0\dot{q}+\Omega^2 q=p(t)/m \tag{41}$$

The error of linearization, a random process, is

$$\text{err}=(\omega_0^2-\Omega^2)q+\beta q^3 \tag{42}$$

which is simply the difference between Eq. (40) and Eq. (41). The method of attack is to minimize the error in a suitable way. The usual choice is to require that the mean-square error $E[\text{err}^2]$ is a minimum, the necessary condition for the requirement is

$$\frac{\partial}{\partial\Omega^2}E[\text{err}^2]=0 \tag{43}$$

If the acoustic pressure excitation $p(t)$ is stationary Gaussian, is ergodic, and has a zero mean, then the approximate displacement q, computed from the linearized Eq. (41), is also Gaussian and approaches stationarity because the panel motion is stable. Substitution of Eq. (42) into Eq. (43) yields

$$(\omega_0^2-\Omega^2)E[q^2]+\beta E[q^4]=0 \tag{44}$$

which leads to the relation between the equivalent linear frequency Ω and the mean-square displacement as

$$\Omega^2=\omega_0^2+3\beta E[q^2] \tag{45}$$

Dividing both sides of Eq. (45) by $(E_2h^2/\rho b^4)$ yields

$$\lambda^2=\lambda_0^2+3\beta^* E[q^2] \tag{46}$$

where $E[q^2]$ is the maximum mean-square deflection of the laminated composite plate.

The mean-square response of modal amplitude from Eq. (41) is

$$E[q^2]=\int_0^\infty S_p(\omega)\,|H(\omega)|^2 d\omega \tag{47}$$

where $S_p(\omega)$ is the PSD function of the excitation $p(t)$. The frequency response function $H(\omega)$ is given by

$$H(\omega)=1/[m(\Omega^2-\omega^2+2i\zeta\omega_0\omega)] \tag{48}$$

For lightly damped ($\zeta\leq 0.05$) structures, the frequency response curves will be highly peaked at Ω (not at ω_0 as in the small-deflection linear theory). The integration of Eq. (47) can be simplified greatly when the spectral density of the excitation is varying slowly in the neighborhood of Ω. Therefore, $S_p(\Omega)$ can be treated as constant in the frequency band surrounding this nonlinear resonance peak Ω. Then, Eq. (47) yields

$$E[q^2]\simeq\frac{\pi S_p(\Omega)}{4m^2\zeta\omega_0\Omega^2} \tag{49}$$

In practice, the PSD function generally is given in terms of the frequency f in Hz. To convert the foregoing result one can substitute $\Omega=2\pi f$ and $S_p(\Omega)=S_p(f)/2\pi$ in Eq. (49). Then, the mean-square peak deflection becomes

$$E[q^2]=32S/\pi^4\zeta\lambda_0\lambda^2, \quad \text{for simply supported plate}$$

$$=32S/81\zeta\lambda_0\lambda^2, \quad \text{for clamped plate} \tag{50}$$

The PSD function $S_p(f)/2\pi$ has the units $(\text{Pa})^2/\text{Hz}$ or $(\text{psi})^2/\text{Hz}$, and S in Eq. (50 is defined as

$$S=\frac{S_p(f)}{\rho^2h^2(E_2h^2/\rho b^4)^{3/2}} \tag{51}$$

G. Solution Procedure

The mean-square displacement $E[q^2]$ in Eq. (49) is evaluated at the equivalent linear frequency Ω, which in turn is related to $E[q^2]$ through Eq. (45). To determine the mean-square deflection, an iterative procedure is introduced. One can estimate the initial mean-square deflection $E[q_0^2]$ using linear frequency ω_0 through Eq. (49) as

$$E[q_0^2]=\frac{\pi S_p(\omega_0)}{4m^2\zeta\omega_0^3} \tag{52}$$

which is simply the mean-square displacement based on linear theory. With this $E[q_0^2]$, a refined estimate of Ω_1 through Eq. (45) is $\Omega_1^2=\omega_0^2+3\beta E[q_0^2]$. Then, $E[q_1^2]$ is computed through Eq. (49) as

$$E[q_1^2]=\frac{\pi S_p(\Omega_1)}{4m^2\zeta\omega_0\Omega_1^2} \tag{53}$$

As the iterative process converges on the nth cycle, the relations

$$E[q_n^2]=\frac{\pi S_p(\Omega_n)}{4m^2\zeta\omega_0\Omega_n^2}\simeq E[q_{n-1}^2] \tag{54}$$

$$\Omega_n^2=\omega_0^2+3\beta E[q_{n-1}^2]\simeq\Omega_{n-1}^2 \tag{55}$$

become satisfied. In the numerical results presented in the following section, convergence is considered achieved when the difference of the rms deflections satisfies the relation

$$\left|\frac{\sqrt{E[q_n^2]}-\sqrt{E[q_{n-1}^2]}}{\sqrt{E[q_n^2]}}\right|\leq 10^{-3} \tag{56}$$

H. Strain and Stress Response

Once the rms displacement is determined, the strains can be obtained from Eqs. (1), (3), and (9). For simply supported angle-ply laminates with immovable inplane edges, the strains on the surface ($z=h/2$) of the plate are

$$\left(\frac{b}{h}\right)^2\epsilon_x=\frac{\pi^2}{r^2}\left\{\left[F_{00}\left(\frac{A_{11}^*r^2}{h}+\frac{A_{12}^*}{h}\right)-\frac{2B_{16}^*r}{h}\right]\sin\frac{\pi x}{a}\sin\frac{\pi y}{b}+\frac{1}{2}\cos\frac{\pi x}{a}\cos\frac{\pi y}{b}\right\}q+\frac{\pi^2}{8}\left(F_{10}A_{12}^*\cos\frac{2\pi x}{a}+F_{01}A_{11}^*r^2\cos\frac{2\pi y}{b}\right)q^2+\frac{\pi^2}{8r^2}q^2 \tag{57a}$$

$$\left(\frac{b}{h}\right)^2\epsilon_y=\frac{\pi^2}{r^2}\left\{\left[F_{00}\left(\frac{A_{22}^*}{h}+\frac{A_{12}^*r^2}{h}\right)-\frac{2B_{26}^*r}{h}\right]\sin\frac{\pi x}{a}\sin\frac{\pi y}{b}+\frac{r^2}{2}\cos\frac{\pi x}{a}\cos\frac{\pi y}{b}\right\}q+\frac{\pi^2}{8}\times\left(\cos\frac{2\pi x}{a}+F_{01}A_{12}^*r^2\cos\frac{2\pi y}{b}\right)q^2+\frac{\pi^2}{8}q^2 \tag{57b}$$

$$\left(\frac{b}{h}\right)^2\gamma_{xy}=\pi^2\left[\left(F_{00}\frac{A_{66}^*}{hr}+\frac{B_{61}^*}{hr^2}+\frac{B_{62}^*}{h}\right)\cos\frac{\pi x}{a}\cos\frac{\pi y}{b}-\frac{1}{r}\sin\frac{\pi x}{a}\sin\frac{\pi y}{a}\right]q \tag{57c}$$

For movable inplane edges, the last term in Eqs. (57a) and (57b) vanishes. Equations for the strain components can also be derived for laminates with clamped edges.

Examining Eqs. (57a-c) leads to a general expression for the strain at any point on the surface of the laminated plate as

$$\epsilon=C_1q+C_2q^2 \tag{58}$$

where the constants C_1 and C_2 can be determined from material properties, dimensions and number of layers of the plate, lamination angle, and the location at which the strain is to be measured. Similarly, by using the stress-strain relations and Eq. (58) yields a general expression for the stress at any point on the surface of the laminate as

$$\sigma=D_1q+D_2q^2 \tag{59}$$

where D_1 and D_2 are constants. The autocorrelation function of the stationary stress is

$$R_{\sigma\sigma}(\tau)=D_1^2E[q(t+\tau)q(t)]+D_2^2E[q^2(t+\tau)q^2(t)]+D_1D_2\{E[q(t+\tau)q^2(t)]+E[q^2(t+\tau)q(t)]\} \tag{60}$$

Under a Gaussian excitation, the approximate $q(t)$ is Gaussian, and Eq. (60) becomes

$$R_{\sigma\sigma}(\tau)=D_1^2R_{qq}(\tau)+D_2^2\{(E[q^2])^2+2R_{qq}^2(\tau)\} \tag{61}$$

where the displacement is assumed to have a zero mean, $E[q(t)]=0$, for simplicity. The mean-square stress (or strain) is then related to the mean-square modal amplitude in a general expression as

$$E[\epsilon^2]=C_1^2E[q^2]+3C_2^2(E[q^2])^2 \tag{62a}$$

$$E[\sigma^2]=D_1^2E[q^2]+3D_2^2(E[q^2])^2 \tag{62b}$$

Therefore, the mean-square stress (or strain) can be obtained from Eq. (62) once the convergence of mean-square displacement, Eqs. (55) and (56), is achieved.

IV. Results and Discussion

Because of the complications in analysis of the many coupled modes, only a single-mode approximation is used in the analysis. The assumption for fundamental mode predominacy is admittedly overly simplified; the conditions under which this is a valid approximation remain to be investigated. This single-mode approximation was first presented by Miles,[20] and its use has become known as "Miles' single degree-of-freedom theory." This approximation commonly is used for all sonic fatigue analyses.[2] Recently, White[21] has showed that the fundamental mode responded significantly and contributed more than 60% to the total mean-square strain response.

In the results presented, the excitation PSD function $S_p(f)$ is considered constant or varying slowly with frequency in the vicinity of the equivalent linear frequency f, and a representative high-modulus graphite-epoxy with material properties

$$E_1/E_2=40 \quad G_{12}/E_2=0.5 \quad \nu_{12}=0.25 \tag{63}$$

is used in all computations. Mean-square displacement, equivalent linear frequency, and mean-square stresses in the principal material directions are determined for rectangular laminates of different length-to-width ratios, lamination angles, number of layers, and panel damping ratios at various nondimensional excitation spectral density parameters.

A. Simply Supported Angle-Ply Plates

In Fig. 2, the rms maximum deflection is given as a function of lamination angle and number of layers for a square an-

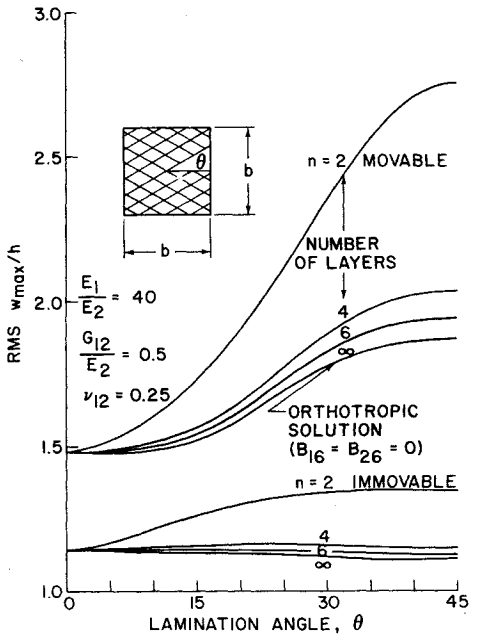

Fig. 2 rms deflection of simply supported square angle-ply plates at $\zeta = 0.02$ and $S = 5000$.

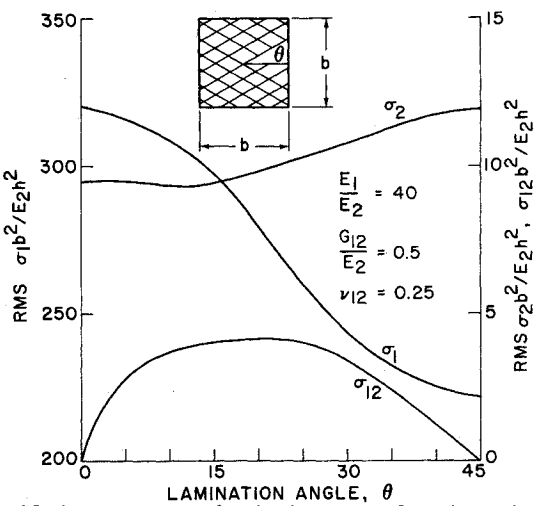

Fig. 3 Maximum rms stress for simply supported two-layered square angle-ply plates with immovable inplane edges at $\zeta = 0.02$ and $S = 5000$.

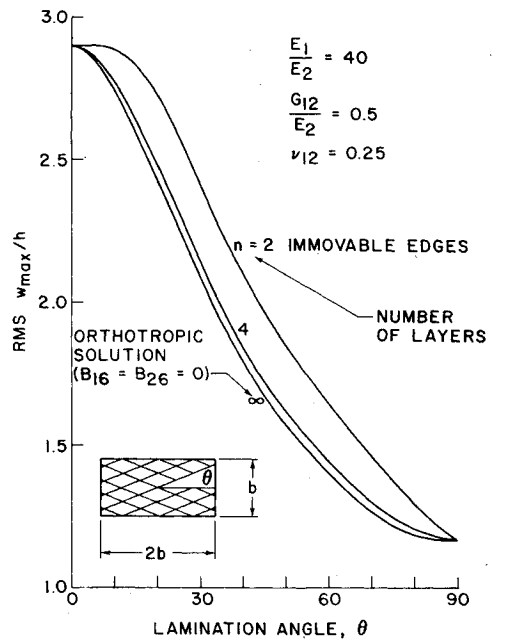

Fig. 4 rms deflection of simply supported rectangular angle-ply plates with immovable inplane edges at $\zeta = 0.02$ and $S = 5000$.

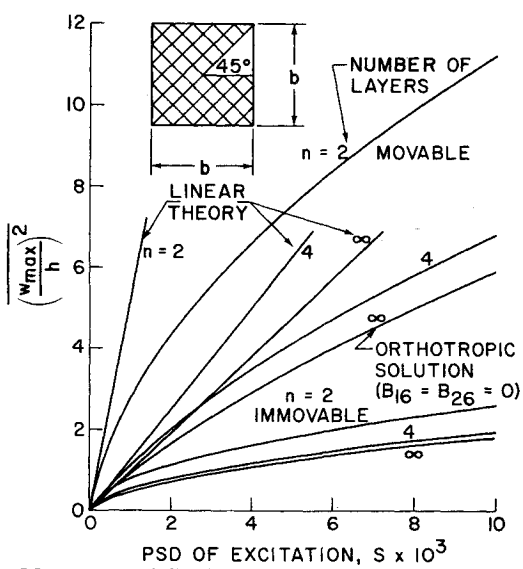

Fig. 5 Mean-square deflection vs pressure spectral density parameter for simply supported square angle-ply plates at $\zeta = 0.02$.

tisymmetric angle-ply laminated graphite-epoxy plate with a damping ratio of $\zeta = 0.02$ and at an acoustic pressure loading with nondimensional spectral density parameter of $S = 5000$. The infinite number of layers case corresponds to the specially orthotropic solution in which the coupling between bending and extension is ignored. For a two-layered plate and a ± 45-deg lamination angle, neglect of coupling results in an underprediction of the deflection by 18 and 32% for immovable and movable inplane edges, respectively. The effect of coupling between bending and extension is quite significant for two-layered laminates, but rapidly decreases as the number of layers increases, irrespective of the lamination angle. For a fixed-laminate thickness h, the bending-extension coupling stiffnesses

$$B_{16}, B_{26} = -(h^2/2n)(\bar{Q}_{16}, \bar{Q}_{26})_{-\theta} \tag{64}$$

obviously decrease as n increases, so the source of the change in the influence of coupling is evident. However, only where there are more than six layers can coupling be ignored without significant error. The rms deflection of the immovable in-plane edges case is much less than that of the movable edges; that is, as the inplane edges are restrained, the plate becomes stiffer.

The normalized rms maximum stresses (at the center of the plate) in the principal material directions vs lamination angle of two-layered square laminates with immovable inplane edges at $\zeta = 0.02$ and $S = 5000$ are shown in Fig. 3. The longitudinal stress component σ_1 decreases very rapidly, but the transverse component σ_2 remains almost constant as θ increases from 0 to 45 deg. The shear stress increases rapidly from zero, then stays constant at $\theta = 10$ to 30 deg, and finally diminishes to zero at $\theta = 45$ deg.

Figure 4 shows the rms deflection as a function of lamination angle and number of layers of a rectangular angle-ply plate of $r = 2$ and a damping ratio 0.02 with immovable edges. The laminates are subjected to an acoustic excitation of spectral density $S = 5000$. Clearly, the effect of coupling between bending and extension is extremely significant for a small number of layers, but it dies out rapidly as the number of layers increases.

The maximum mean-square deflections vs nondimensional spectral density parameter of acoustic pressure excitation for a square plate with a ± 45-deg lamination angle are shown in Fig. 5. Clearly, coupling is significant for two-layered

laminates, but rapidly decreases as the number of layers increases. The mean-square deflections of the movable inplane edges cases are approximately three to four times those of the immovable edges. Results of mean-square deflection vs forcing spectral density based on small deflection theory are also shown. The use of linear theory would lead to poor prediction of fatigue life.

B. Clamped Angle-Ply Plates

In Fig. 6, the rms maximum deflection is shown as a function of lamination angle and number of layers for a square angle-ply plate with $\zeta = 0.02$ and subjected to a pressure excitation $S = 5000$. The rms deflection increases with the lamination angle. The presence of coupling between bending and extension generally increases deflections. For example, the rms deflection of a clamped square plate with $\theta = 45$ deg and 2 layers is about 50% more than the specially orthotropic solution which is valid when the number of layers is infinite. Again, as the number of layers increases, the effect of coupling decreases. The rms deflection of the clamped plates is generally somewhat less than that of the simply supported case.

The rms deflection results as a function of lamination angle and number of layers for a rectangular angle-ply plate of aspect ratio $r = 2$ and a damping ratio 0.02 with immovable inplane edges are shown in Fig. 7. The rms deflection decreases very rapidly as the lamination angle increases, which has completely different characteristics as compared with the square plate.

In Figs. 8 and 9, the mean-square deflection vs PSD of excitation is given for a square plate with $\theta = \pm 35$ deg and a rectangular ($a/b = 2$) plate with $\theta = \pm 30$ deg, respectively. The mean-square deflection of the movable inplane edges case is only approximately twice that of the immovable edges case. The difference of mean-square deflections between immovable and movable edges for clamped laminates is small compared to that for simply supported laminates. Results based on linear structural theory are also given in the figures.

Figure 10 shows the rms deflection vs lamination angle for clamped square six-layered angle-ply plates of different

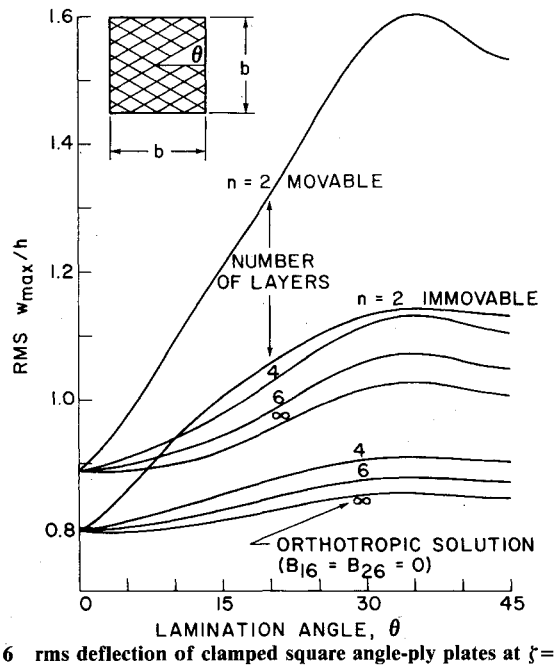

Fig. 6 rms deflection of clamped square angle-ply plates at $\zeta = 0.02$ and $S = 5000$.

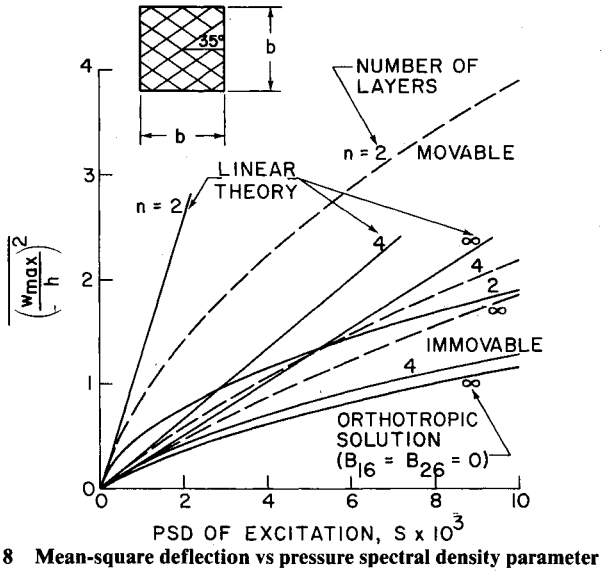

Fig. 8 Mean-square deflection vs pressure spectral density parameter for clamped square angle-ply plates, $\zeta = 0.02$.

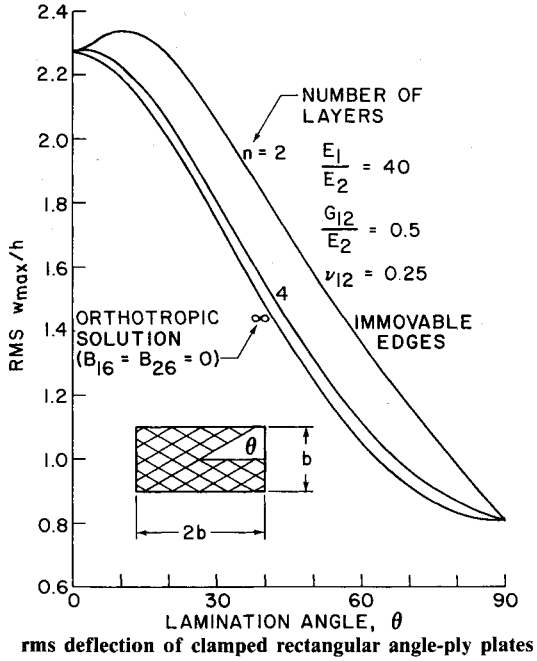

Fig. 7 rms deflection of clamped rectangular angle-ply plates with immovable inplane edges at $\zeta = 0.02$ and $S = 5000$.

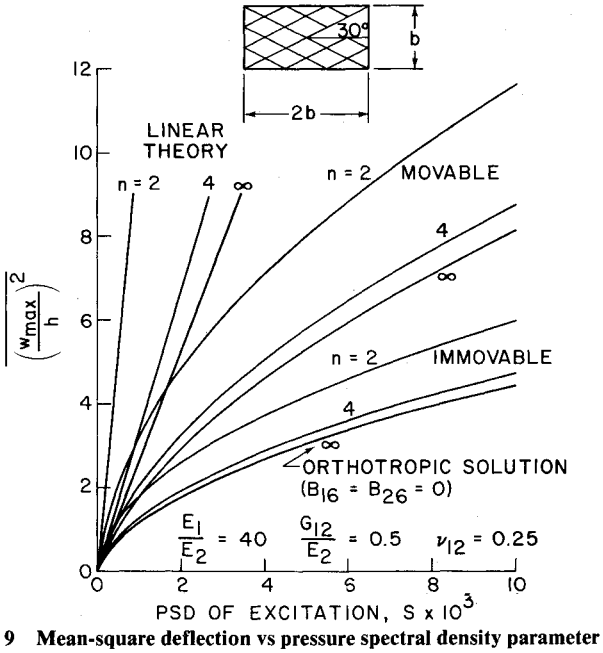

Fig. 9 Mean-square deflection vs pressure spectral density parameter for clamped rectangular angle-ply plates, $\zeta = 0.02$.

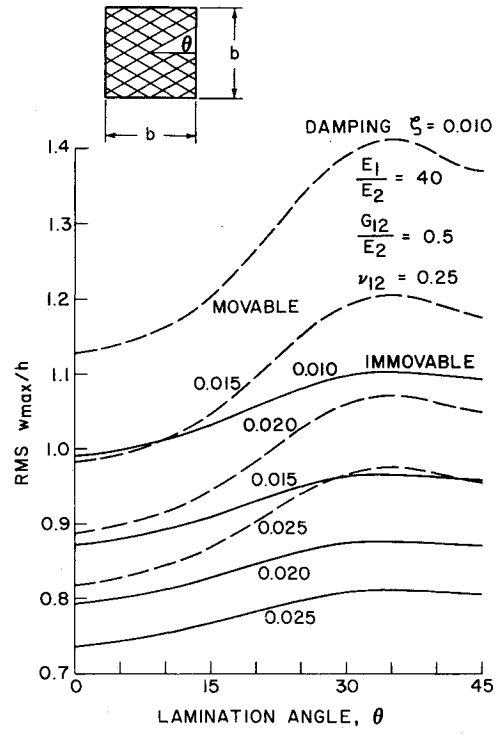

Fig. 10 Effects of damping on rms deflection for clamped square six-layered angle-ply plates at $S = 5000$.

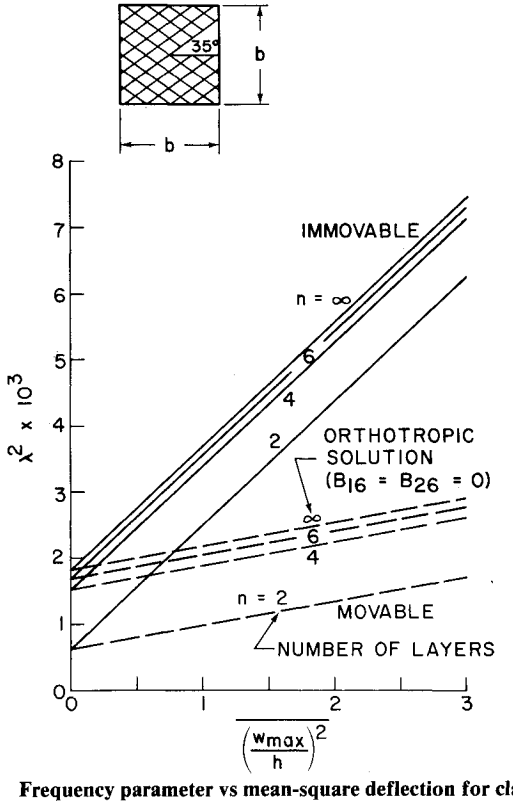

Fig. 11 Frequency parameter vs mean-square deflection for clamped square angle-ply plates.

damping ratios. It is clear from the figure that the precise determination of plate damping is important.

In Fig. 11, the equivalent linear frequency square vs mean-square deflection for a square plate with $\theta = \pm 35$ deg is given. The frequencies corresponding to zero mean-square deflection are resonance frequencies based on linear structural theory. The equivalent linear frequency should be used in estimation of panel fatigue life. Clearly, the use of frequency obtained from linear theory will give poor estimation.

V. Concluding Remarks

An analytical method is presented for determining large-amplitude response of antisymmetric angle-ply laminated rectangular plates subjected to broadband random acoustic excitation. Governing equations in terms of a stress function and the deflection function are derived. The formulation is based on the Karman-type geometric nonlinearity, a single-mode Galerkin approach, the equivalent linearization method, and an iterative procedure. Angle-ply laminates of both simply supported and clamped support conditions with either immovable or movable inplane edges are considered. Computer programs are developed to aid in the determination of rms deflection, rms stress/strain, and equivalent linear frequency at given pressure spectral density of excitation. This computed rms stress/strain and equivalent linear frequency, in conjunction with failure S-N data, should be used for the estimation of service life. Experiments on simple composite plates are needed urgently for adequate quantitative comparison. The test measurements should include linear frequency, equivalent linear or nonlinear frequency, damping ratio, rms deflection, rms strains, and excitation pressure spectral density.

The presence of coupling between bending and extension in a laminate generally increases rms deflections and rms stresses. Hence, coupling decreases the effective stiffnesses of a laminate. The effect of coupling, however, dies out rapidly as the number of layers increases. For more general laminates, specific investigation is required.

Acknowledgments

This work was sponsored by the Air Force Office of Scientific Research, Air Force Systems Command, under Grant AFOSR-80-0107.

References

[1] Mei, C., "Response of Nonlinear Structural Panels Subjected to High Intensity Noise," Wright Patterson Air Force Base, Ohio, AFWAL-TR-80-3018, March 1980.

[2] Rudder, F. F. Jr. and Plumblee, H. E. Jr., "Sonic Fatigue Design Guide for Military Aircraft," Wright Patterson Air Force Base, Ohio, AFFDL-TR-74-112, May 1975.

[3] Volmir, A. S., "The Nonlinear Dynamics of Plates and Shells," Wright Patterson Air Force Base, Ohio, Foreign Technology Div., AD-781338, April 1974, Chap. X.

[4] Thomson, A.G.R. and Lambert, R. F., "Acoustic Fatigue Design Data," NATO Advisory Group for Aeronautics Research and Development, AGARD-AG-162, Pt. I and II, 1972.

[5] Jacobs, L. D. and Lagerquist, D. R., "Finite Element Analysis of Complex Panel to Random Loads," Wright Patterson Air Force Base, Ohio, AFFDL-TR-68-44, Oct. 1968.

[6] Fox, H. L., Smith, P. W. Jr., Pyle, R. W., and Nayak, P. R., "Contributions to the Theory of Randomly Forced, Nonlinear, Multiple-Degree-of-Freedom, Coupled Mechanical Systems," Wright Patterson Air Force Base, Ohio, AFFDL-TR-72-45, Aug. 1973.

[7] Holehouse, I., "Sonic Fatigue Design Techniques for Advanced Composite Aircraft Structures," Wright Patterson Air Force Base, Ohio, AFWAL-TR-80-3019, April 1980.

[8] Wentz, K. R. and Wolfe, H. F., "Development of Random Fatigue Data for Adhesively Bonded and Weldbonded Structures Subjected to Dynamic Excitation," *ASME Journal of Engineering Materials and Technology*, Vol. 100, Jan. 1978, pp. 70-76.

[9] Jacobson, M. J., "Sonic Fatigue Design Data for Bonded Aluminum Aircraft Structures," Wright Patterson Air Force Base, Ohio, AFFDL-TR-77-45, June 1977.

[10] Van der Heyde, R.C.W. and Wolf, N. D., "Comparison of the Sonic Fatigue Characteristics of Four Structural Designs," Wright Patterson Air Force Base, Ohio, AFFDL-TR-76-66, Sept. 1976.

[11] Van der Heyde, R.C.W. and Smith, D. L., "Sonic Fatigue Resistance of Skin-Stringer Panels," Wright Patterson Air Force Base, Ohio, AFFDL-TM-73-149-FYA, April 1974.

[12] Jacobson, M. J., "Advanced Composite Joints; Design and Acoustic Fatigue Characteristics," Wright Patterson Air Force Base, Ohio, AFFDL-TR-71-126, April 1972.

[13] Caughey, T. K., "Equivalent Linearization Techniques," *Journal of the Acoustical Society of America*, Vol. 35, Nov. 1963, pp. 1706-1711.

[14] Caughey, T. K., "Nonlinear Theory of Random Vibrations," *Advances in Applied Mechanics*, Vol. 11, edited by C. S. Yih, Academic Press, 1971, pp. 209-253.

[15] Spanos, P.T.D. and Iwan, W. D., "On the Existence and Uniqueness of Solutions Generated by Equivalent Linearization," *International Journal of Non-Linear Mechanics*, Vol. 13, No. 2, 1978, pp. 71-78.

[16] Jones, R. M., *Mechanics of Composite Materials*, McGraw Hill, 1975.

[17] Tsai, S. W. and Hahn, H. T., *Introduction to Composite Materials*, Technomic Publishing, 1980.

[18] Almroth, B. O., "Influence of Edge Conditions on the Stability of Axially Compressed Cylindrical Shells," *AIAA Journal*, Vol. 4, Jan. 1966, pp. 134-140.

[19] Rupert, C. L. and Wolf, N. D., "Sonic Fatigue and Response Tests of Boron Composite Panels," Wright Patterson Air Force Base, Ohio, AFFDL-FYA-73-10, July 1973.

[20] Miles, J. W., "On Structural Fatigue Under Random Loading," *Journal of the Aeronautical Sciences*, Vol. 21, Nov. 1954, pp. 753-762.

[21] White, R. G., "Comparison of the Statistical Properties of the Responses of Aluminum Alloy and CFRP Plates to an Acoustic Excitation," *Journal of Composite Materials*, Oct. 1978, pp. 251-258.